Ecological Indicators 121 (2021) 106999

Contents lists available at ScienceDirect

Ecological Indicators

journal homepage: www.elsevier.com/locate/ecolind

EOLakeWatch; delivering a comprehensive suite of remote sensing algal bloom indices for enhanced monitoring of Canadian eutrophic lakes

C.E. Binding *, L. Pizzolato, C. Zeng

Water Science and Technology Directorate, Environment and Climate Change Canada, 867 Lakeshore Rd, Burlington, Ontario L7S 1A1, Canada

ARTICLE INFO

Keywords:
Algal blooms
Cyanobacteria
Remote sensing
Lake water quality

ABSTRACT

Early detection and comprehensive monitoring of inland water algal blooms is fundamental to their effective management and mitigation of potential ecosystem and public health impacts. With the spatial and temporal limitations of in situ sampling, algal bloom monitoring capabilities have been enhanced greatly by advancements in satellite Earth Observation (EO). Three turbid, eutrophic Canadian lakes (Lake Winnipeg (LW); Lake Erie (LE); Lake of the Woods (LoW)) have been the focus of Environment and Climate Change Canada (ECCC) research and monitoring initiatives due to concerns over persistent degraded water quality from recurring algal blooms. ECCC's EOLakeWatch was developed to deliver a suite of useful, easily interpretable, and accessible EO-derived products to support algal bloom monitoring on these three lakes. Algal bloom indices, describing bloom spatial extent, intensity, duration, and severity were derived using the European Space Agency's OLCI (Ocean and Land Colour Instrument) sensor for observations from 2016 to present and its predecessor MERIS (Medium Resolution Imaging Spectrometer) for 2002 to 2011. Results document widespread blooms on each lake, with maximum spatial extent of 21,641 km^2 (representing 88.1% of the lake area) on LW, 3070 km^2 (79.5%) on LoW and 5257 km^2 (19.7%) on LE. Bloom intensity showed seasonal and inter-annual variability on all three lakes, with a suggestion that LoW may be responding to reduced nutrient loads with a recent decrease in bloom intensity. Annual bloom duration on LW and LoW was on average 44 and 47 days respectively, while on LE blooms were significantly shorter in duration at an average of 24 days. Variance among the derived bloom indices was shown to be significant (i.e. the most extensive bloom was not necessarily the longest or most intensive), demonstrating the need for the indices to be used collectively, or for any single comprehensive bloom indicator to capture the variability of all individual metrics. Bloom indices are processed in a fully automated operational capacity, distributed in near-real-time through a web portal and collated into end-user-friendly annual algal bloom reports for each lake. These products go a long way to address existing monitoring gaps, delivering prompt, consistent measures of lake-wide algal bloom conditions required to provide stakeholders with early warning of bloom risks, identify areas of potential concern, quantify spatio-temporal trends, further understand bloom dynamics and drivers, as well as guide and determine the effectiveness of implemented management actions.

1. Introduction

There is substantial evidence that the frequency and magnitude of harmful algal blooms (HABs) in coastal and inland waters around the world have been increasing, attributed in large part to cultural eutrophication, and climate change (Hallegraef, 1993; Glibert et al., 2005; Paerl and Huisman, 2008; Heisler et al., 2008). Likewise, many freshwater systems in Canada have seen increases in HAB occurrences, posing serious threats to ecosystem integrity and significant public health risks (Kling, 1998; Watson et al., 2008; Winter et al., 2011; Stumpf et al., 2012; Pick, 2016). The proliferation of inland water HABs has a multitude of impacts on ecosystem services; from drinking water resources, commercial fisheries, leisure and recreational activities, and the generation of hydroelectric power, leading to significant socio-economic costs when a waterbody is rendered unsuitable for its wide-ranging uses (Smith et al., 2019). In most regions of North America the majority of freshwater planktonic HABs are caused by cyanobacteria (Watson et al., 2016; Lopez et al., 2008). Several cyanobacteria taxa have the capacity to produce potent toxins that can cause a range of hepatic, neurologic and dermatologic effects, therefore raising serious health concerns when

* Corresponding author.
E-mail address: Caren.Binding@canada.ca (C.E. Binding).

https://doi.org/10.1016/j.ecolind.2020.106999
Received 6 July 2020; Received in revised form 16 September 2020; Accepted 21 September 2020
Available online 2 October 2020

they are detected in recreational or drinking water resources (Miller et al., 2017). HABs lower the aesthetic value of waterbodies and by reducing water clarity impact light availability for pelagic and benthic ecosystems. Upon senescence, blooms contribute to hypolimnetic hypoxia, causing disruption and mortality to pelagic and benthic biological communities (Watson et al., 2016).

Three large lakes in Canada (Lake Winnipeg, Lake of the Woods and Lake Erie (Fig. 1) have been the focus of Environment and Climate Change Canada (ECCC) research and monitoring initiatives under the Action Plan for Clean Water because of concerns over persistent degraded water quality due to recurring algal blooms. Lake Winnipeg (LW) is Canada's sixth largest lake (Fig. 1B); it is a shallow, turbid lake, covering an area of 23,750 km^2 with a watershed spanning almost a million square kilometers. LW has experienced accelerated nutrient loading and a dramatic increase in phytoplankton biomass over the last two decades brought about by intensified agricultural practices and livestock production, urban development, and changing hydrology (Kling et al., 2011; Schindler et al., 2012; McCullough et al., 2012; Bunting et al., 2016). Blooms on LW have been reported to consist primarily of non nitrogen-fixing cyanobacteria (several species of *Microcystis* and *Planktothrix*) in the south basin, with the north basin exhibiting reduced taxonomic diversity with a predominance of the nitrogen-fixing cyanobacteria *Aphanizomenon flosaquae* and *Dolichospermum* spp. (Kling et al., 2011). Through the Lake Winnipeg Basin Program (LWBP), ECCC has supported local stewardship action, monitoring, and research activities, to address the impacts of nutrient enrichment and inform watershed-based nutrient-reduction strategies. Targets have been set to reduce phosphorus levels by 50% in an effort to restore lake conditions to a pre-1990 state and reduce the frequency and severity of algal blooms (ECCC, 2013).

Lake of the Woods (LoW), draining into LW via the Winnipeg River, is an international water body spanning the Canadian Provinces of Ontario and Manitoba and the U.S. state of Minnesota. Covering an area over 3850 km^2, LoW is a hydrologically complex lake, consisting of an expansive, shallow and well-mixed bay to the south and a collection of deeper, occasionally stratified interconnected basins and ~14,500 islands to the north (Fig. 1C). LoW has been under significant water quality pressures due to historical nutrient over-enrichment from industrial pulp and paper and domestic sewage facilities (DeSellas et al., 2009; Anderson et al., 2017). Blooms on LoW have typically been dominated by *Aphanizomenon* except in the deeper northern embayments, where *Dolichospermum* often predominates (Watson and Kling, 2017). Despite reductions in Total Phosphorous loads in the last few decades, symptoms of eutrophication persist, manifested by ongoing severe cyanobacteria blooms (Anderson et al., 2017) which frequently cover as much as 80% of the lake's surface (Binding et al., 2011). Exacerbating factors such as warming temperatures and legacy nutrients stored in sediments are postulated to have, so far, limited a full recovery of the lake (Paterson et al., 2017; Reavie et al., 2017). Recently the International Joint Commission (IJC, 2018) endorsed a recommendation by the International Rainy – Lake of the Woods Watershed Board to create binational phosphorus load reduction targets for the lake after the Minnesota portion of LoW was declared impaired for recreational use due to exceedances of eutrophication criteria (Heiskary and Wilson, 2008).

Lake Erie (LE) is the shallowest and most biologically productive of North America's Laurentian Great Lakes, and has seen a proliferation of scientific and media attention in the last decade due to a resurgence of algal blooms (Watson et al., 2016). Binational efforts in the 1970's to reduce phosphorous loadings to the lake led to significant declines in phytoplankton biomass but since the early 2000's, cyanobacteria blooms have once again become a recurring annual event, particularly across the western basin of LE. Blooms are often reported as heavily dominated by the potentially toxic cyanobacterium *Microcystis* (Bridgeman et al., 2013; Michalak et al., 2013; Steffen et al., 2014) although others have indicated that the bloom consists of a more diverse community composition (Berry et al., 2016; Davis et al., 2015; Moore et al., 2017; Binding et al., 2019). The algal bloom of 2014 led to the City of Toledo issuing a drinking water advisory to more than 400,000 residents due to the presence of unsafe levels of the toxin Microcystin (Jetoo et al., 2015). Renewed commitment to remedial action with the amended Great Lakes Water Quality Agreement (GLWQA) led to binational adoption of targets for a 40% reduction in phosphorus loads compared to a 2008 baseline in order to meet Lake Ecosystem Objectives of levels of algal biomass, species composition and toxin concentrations consistent with a healthy aquatic ecosystem (GLWQA, 2012; Baker et al., 2019).

To varying extents, in situ water quality monitoring is conducted on all three lakes by federal, provincial and municipal levels of government as well as academic partners. However, blooms vary from localized to lake-wide events and can be highly dynamic in space and time therefore are difficult to adequately capture with conventional sampling methods

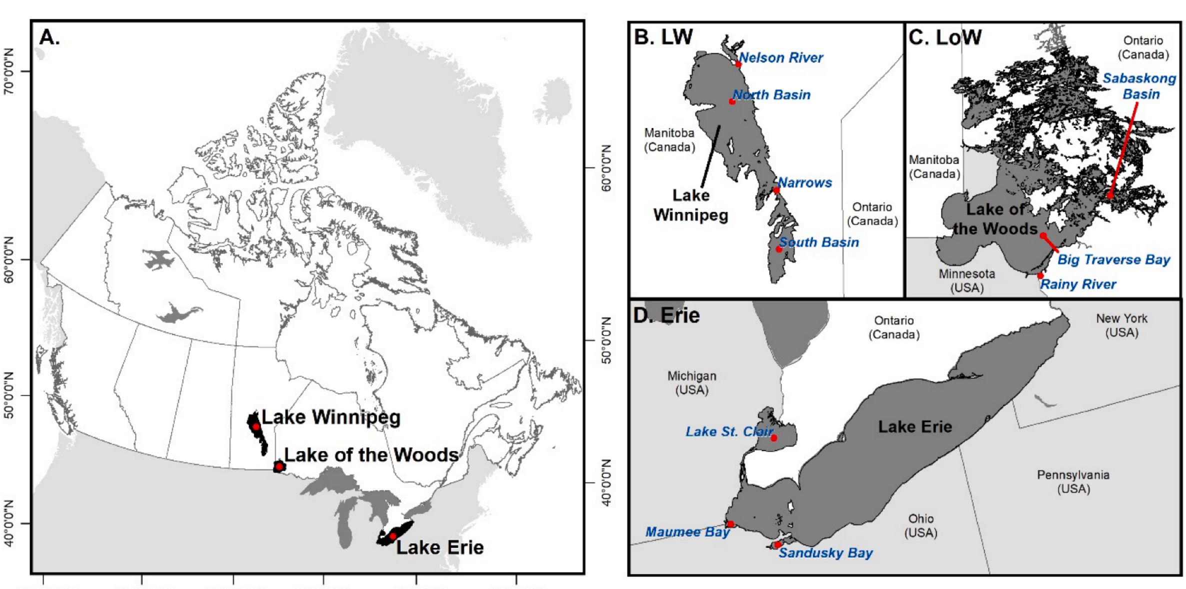

Fig. 1. (A) Map of Canada's largest inland waters identifying the key lakes of interest in this study: (B) Lake Winnipeg (C) Lake of the Woods and (D) Lake Erie.

collecting discrete water samples (Kutser et al., 2006; Reinart and Kutser, 2006; Kahru et al., 2007). Even with regular monitoring programs, reliable spatio-temporal analyses are often hampered by fragmented datasets (Dove and Chapra, 2015; Kratzer et al., 2019), while inconsistencies in the timing of surveys make multi-lake or multi-year comparisons a challenge. This lack of consistent, large-scale, time-series data on the severity of blooms often impedes resolving short- and long-term variance in HAB events and developing robust management strategies for their mitigation.

Earth observation (EO) satellites providing multi- or hyper-spectral observations of inland water colour enable quantitative assessment of algal biomass via estimates of chlorophyll-a concentrations. Beyond chlorophyll retrievals, EO has been used to deliver quantitative measures of algal bloom intensity and severity (Stumpf et al., 2012), spatial extent (Urquhart et al., 2017), and frequency (Clark et al., 2017). The benefits of EO are unequivocal; providing low-cost, frequent, large-scale synoptic observations of HAB events simply not possible using ground-based monitoring networks. A demonstrable confidence in EO-derived algal bloom measures, along with improvements in data access and image processing capabilities with modern computational power allowing for near-real-time product delivery, have led to an increase in the adoption of EO products for research, monitoring and policy development. Satellite observations have increasingly been integrated operationally into inland water algal bloom monitoring, providing public information and early warning services, through programs such as the U.S. National Oceanic and Atmospheric Administration (NOAA) HAB Tracker (Stumpf et al., 2016a), the U.S. Environmental Protection Agency (EPA) CyAN project (Schaeffer et al., 2018), CyanoTRACKER (Mishra et al., 2020) and CyanoLakes (Matthews, 2016). EO also forms a key component of Baltic Sea cyanobacterial bloom monitoring, combining estimates of the areal coverage, duration and bloom severity into the Cyanobacterial Bloom Index (CyaBI) as a core eutrophication indicator to evaluate the current bloom status in relation to historical target conditions (Kahru and Elmgren, 2014; Anttila et al., 2018). A key challenge in distributing operational satellite-derived water quality information to a wide range of stakeholders lies in distilling large volumes of complex EO data into useful, readily interpretable, and accessible end-user products. In June 2020 ECCC launched EOLakeWatch to deliver a suite of EO-derived algal bloom products of value to water resource stakeholders and the public, and support inland water HAB monitoring and research activities. EOLakeWatch builds on ECCC's previous work developing and validating algorithms for remote sensing of algal blooms (Binding et al., 2011, 2013, 2018, 2019) to transition to an operational service delivery. Products are distributed in near-real-time through a web-based data portal (EOLakeWatch, 2020) and collated into annual algal bloom reports for each lake for distribution to interested stakeholders (see Fig. 2 for example report). Data contributing to the EOLakeWatch portal and annual bloom reports are also accessible via the Government of Canada's open data catalogue (ECCC, 2020).

In this manuscript, we present: (1) a description of the EOLakeWatch image processing workflow and the suite of indices produced for algal bloom monitoring on LW, LoW, and LE, (2) documentation of bloom intensity, spatial extent, duration and severity on each lake since 2002, and (3) an analysis of variability among those indices in capturing bloom conditions on each lake. Results are discussed in the context of water quality monitoring and management needs and in further understanding environmental drivers of blooms.

2. Methods

2.1. Image processing workflow

Algal bloom products were derived using data from the Ocean and Land Colour Instrument (OLCI) on the European Space Agency's (ESA) Sentinel-3A satellite, launched in February 2016, and its predecessor the Medium Resolution Imaging Spectrometer (MERIS) on board ESA's Envisat, which operated from 2002 to 2011. The image processing

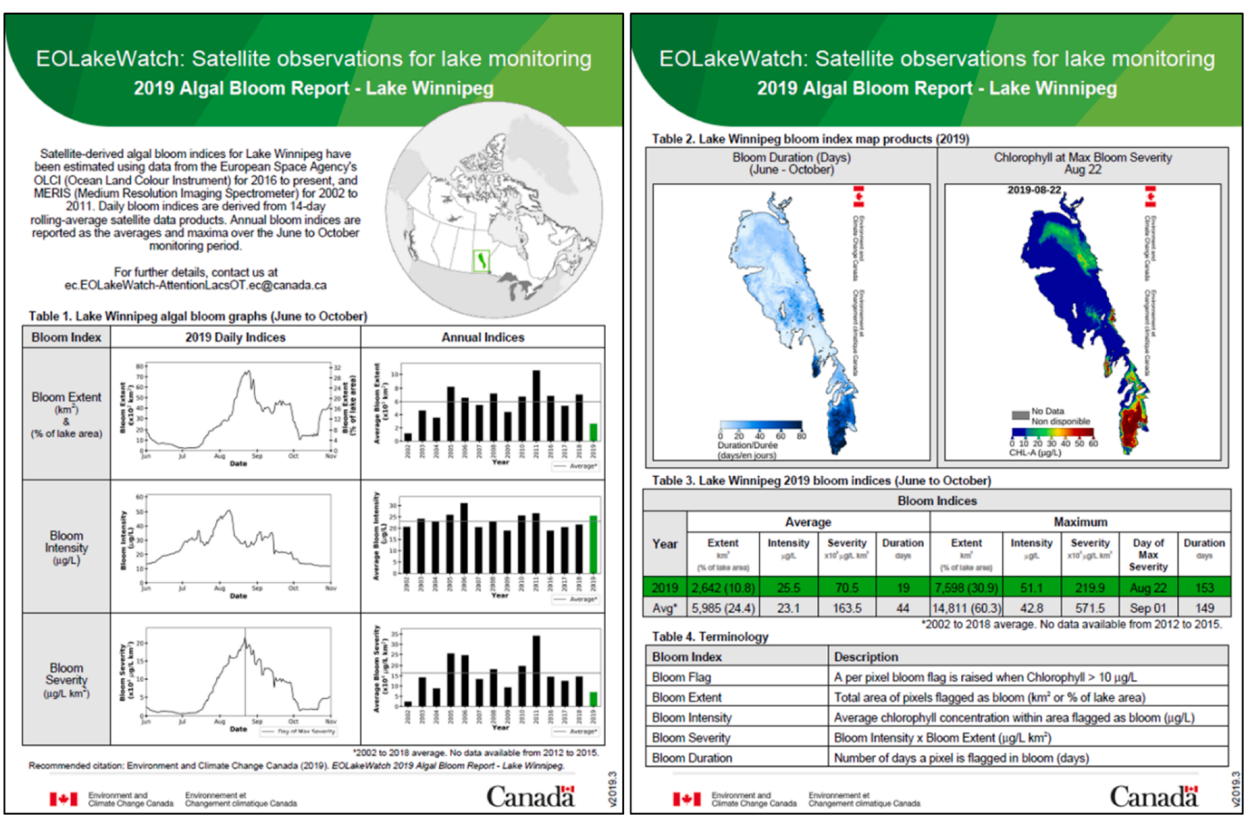

Fig. 2. ECCC's EOLakeWatch 2019 annual algal bloom report for Lake Winnipeg.

workflow (Fig. 3) begins with the automated download of OLCI Level-1 FR (full resolution, 300 m spatial resolution at nadir) imagery from the Copernicus Open Access Hub on a daily basis from June 1 to October 31. MERIS Level-1 FR imagery were obtained from ESA's MERCI online archive (www.merisfrs-merci-ds.eo.esa.int). The June to October window captures the majority of the cyanobacteria bloom season on all three lakes, is in line with peak recreational usage and potential socio-economic impact, and minimizes potential image artifacts brought about by winter lake ice cover. Fully automated image processing routines were developed, with customised scripts in Python, ESA's SNAP and QGIS, running on Ubuntu OS. True colour quick-view images are produced and reviewed for quality assurance. Top-of-atmosphere spectral radiance (L(λ)), georeferenced and calibrated to geophysical units ($W/m^2/sr/\mu m$), are subset to defined regions of interest for each lake. Images are masked according to quality flags (sun glint, duplicate pixels, bright, coastline, or otherwise invalid pixels). Chlorophyll retrieval algorithms exploiting the Red-NIR portion of the spectrum perform well in turbid eutrophic waters (Gilerson et al., 2010) and line-height algorithms such as the Maximum Chlorophyll Index (MCI: Gower et al., 2008), are particularly favourable due to their relative insensitivity to uncertainties in atmospheric correction. The MCI, quantifies a peak in radiance at 708 nm relative to a baseline interpolated between bands either side, capturing the red-edge reflectance feature associated with dense surface algal blooms. MCI, MCI_slope and Chlorophyll-a concentrations (Chla) are calculated according to Eqs. (1), (2) and (3) respectively. MCI_slope is used to mask extreme sediment events, which have been shown to lead to potential false positive bloom detection in red-NIR line-height based algorithms (Zeng and Binding, 2019).

$$\mathrm{MCI} = \mathrm{L}(\lambda_2) - \mathrm{L}(\lambda_1) - \frac{\lambda_2 - \lambda_1}{\lambda_3 - \lambda_1}\cdot[\mathrm{L}(\lambda_3) - \mathrm{L}(\lambda_1)] \quad (1)$$

$$\mathrm{MCI\_slope} = \frac{\mathrm{L}(\lambda_3) - \mathrm{L}(\lambda_1)}{\lambda_3 - \lambda_1} \quad (2)$$

$$\mathrm{Chla} = 6.166.\mathrm{MCI} + 6.347 \quad (3)$$

where for both OLCI and MERIS, λ_1, λ_2 and λ_3 are centered at 681, 708, and 753 nm respectively. Daily Chla images are created and combined into rolling 14-day average (14d_avg) Chla images. The algal bloom flag is raised on a pixel by pixel basis when Chla is in excess of 10 µg/L. This threshold follows the World Health Organization guideline levels, for relatively mild/low probabilities of adverse health effects, of 20,000 cells/mL (corresponding to 10 µg/L of Chla under conditions of cyanobacterial dominance). This threshold is also consistent with the approximate Chla above which most algorithms in the red-NIR are sensitive (Moses et al., 2009; Binding et al., 2013). With the same spectral and spatial resolution, the continuity in sensor specifications offered by MERIS and OLCI allow for consistent bloom retrievals for the period 2002–2011 and 2016 to present. There exists, however, a significant data gap over the years 2012–15 for which sensors with the required spectral configuration for the MCI are not available and therefore indices for those years are not reported here.

2.2. Algal bloom indices

All algal bloom indices are measured only on those pixels flagged as in bloom (i.e. Chla greater than 10 µg/L). Bloom statistics are extracted on a daily basis on both the 14d_avg and daily composite images, as follows:

- ***Bloom Intensity*** (µg/L) is determined as the average Chla within the area flagged as in bloom.
- ***Bloom Extent*** (km^2 or % of lake area) is measured as the total number of pixels flagged as in bloom. The number of bloom pixels multiplied by 0.09 (the 0.03 km × 0.03 km resolution of each pixel at nadir) gives the bloom extent in km^2. Dividing the number of bloom pixels by the total number of lake pixels gives the extent as a % of lake area.
- **Bloom Severity** (µg/L km^2) is determined as the product of Bloom Intensity and Extent, therefore representing the total surface Chla over the bloom area.
- ***Bloom Duration*** is calculated on a per pixel basis and mapped daily as a cumulative count from the start of the monitoring period (June 1st). Duration is linearly interpolated temporally between cloud-free dates; for any given cloud-masked pixel the bloom is assumed present throughout the cloudy period (and added to the cumulative bloom duration) if the bloom flag is raised on dates either side of the cloud period. For pixels where the bloom flag is raised only on one of the dates (before or after cloud cover), the bloom is assumed present for half that period. Cumulative bloom duration images are output daily such that the bloom duration image of October 31st represents the whole season June through October.
- **Annual Bloom Indices** are calculated as the average and maximum of daily indices (intensity, extent, severity) over the June to October monitoring season. The annual average bloom duration is extracted from the October 31st duration image as the average of all pixels greater than zero (representing an average bloom duration for the

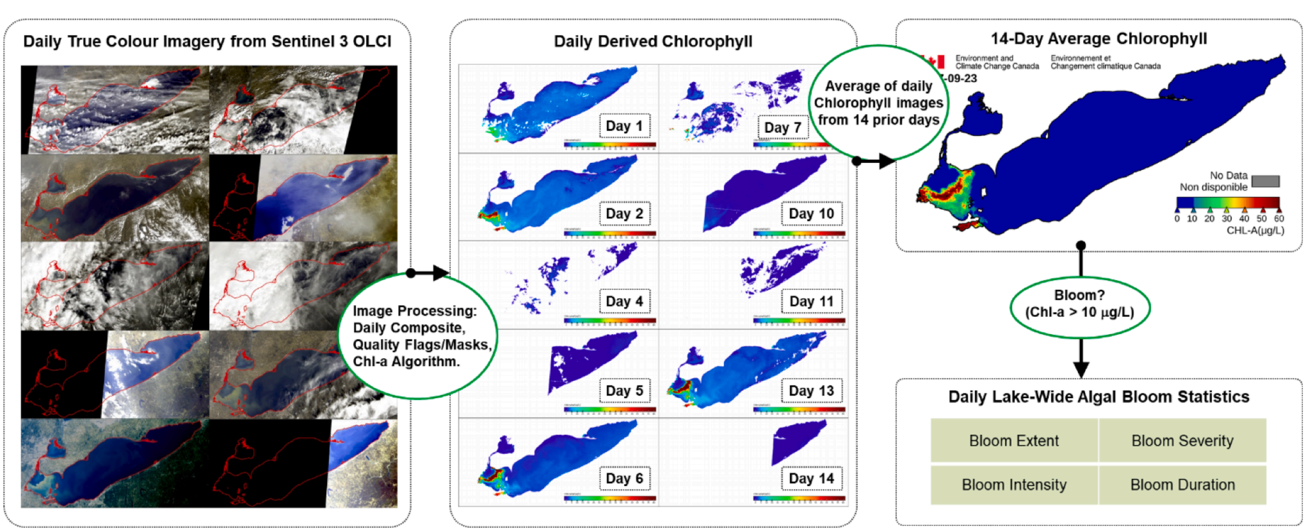

Fig. 3. ECCC's Sentinel-3 OLCI algal bloom products image processing workflow.

total area where a bloom was detected at least once over the bloom season).

3. Results

3.1. Satellite data coverage and temporal binning

The potential number of satellite observations for all three lakes is extensive, with ~300,000, ~270,000 and ~43,000 pixels at 300 × 300 m spatial resolution over LE, LW and LoW respectively. However, partial swaths, cloud cover, lake-ice, and several quality masks reduce the frequency of useable data for any given pixel. Each pixel provided an average of 42, 36 and 44 cloud-free valid observations for LE, LW and LoW respectively over the June to October time period. This spatial and temporal coverage is a stark improvement over the capabilities of in situ monitoring even for the most frequently monitored lakes. As shown in Fig. 4, however, the daily spatial coverage on any single satellite scene varies considerably. For example, in 2010 for MERIS the average spatial coverage of daily scenes was just 48%, 31% and 58% of lake area for LE, LW and LoW respectively, while for OLCI in 2017 average spatial coverage was 47%, 41%, and 63%. Consequently, despite the considerable number of observations, one of the greatest challenges to accurately delineating and quantifying bloom spatial extent and intensity is in dealing with loss of data over individual scenes.

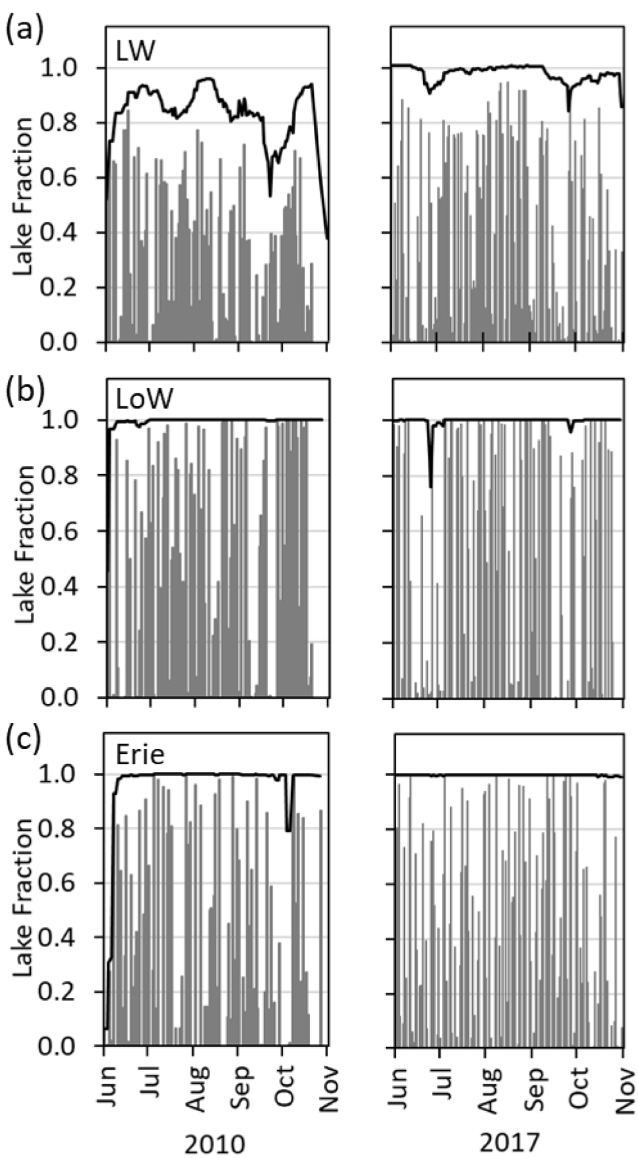

Fig. 4. Number of valid pixels over the June to October monitoring seasons for MERIS in 2010 and OLCI in 2017, represented as a fraction of total lake area per day for each lake. Bold line represents the average daily percentage coverage for the 14-day rolling average (14d_avg) products.

Bloom statistics calculated on individual daily scenes result in large day-to-day variability (Fig. 5 shows 2017 daily bloom intensity and spatial extent for example). This variability is primarily due to bias introduced by data gaps originating from cloud cover and/or quality flag masking, as well as spatio-temporal variations in surface bloom conditions brought about by advection, growth/senescence and wind driven mixing. Using a data coverage threshold to select useable images may be valuable; the number of scenes between June and October 2017 with >70% valid data by area was 38, 38 and 54 for LE, LW and LoW respectively. However, the remaining 30% of any individual scene may mask the most intense portion of the bloom, leading to skewed bloom statistics. Conversely, an image with less than 70% valid data may adequately capture the maximum extent of a localised bloom. Hence even with 70% coverage imagery there is significant day-to-day variability in bloom intensity and extent brought about by data availability artifacts (Fig. 5). Furthermore, spatial coverage of daily imagery often has a seasonal bias; for example on LoW, cloud-free images were more frequently captured in July and August (fraction of images with >70% spatial coverage: Jun = 13%, Jul = 30%, Aug = 26%, Sep = 21%, Oct = 11%). Using bloom indices derived from daily images would therefore require *a priori* knowledge of cloud cover and bloom location, a hindrance to the fully automated large scale monitoring potential that remote sensing offers.

To address these data gaps and potential biases, the adopted workflow produces rolling average composite Chla images. To provide a product that offers consistency for the reduced data availability during the MERIS mission, we currently opt for a 14-day rolling average product (14d_avg), which results in near complete lake coverage for all three lakes (Fig. 4). LW still exhibits a lower usable data rate than LoW and LE due to frequent extreme turbidity events that raise quality flags in this shallow well mixed lake. The 14d_avg product adequately captures the maximum extent of the bloom without the day-to-day variability brought about by data gaps (Fig. 5). For bloom intensity, while it is acknowledged a rolling average will smooth out peak Chla concentrations, it also removes much of the bias introduced by partial images and day-to-day variability from wind mixing events, therefore providing a consistent measure for trend detection. Wind-induced water column mixing can prevent the bloom from rising to the surface, resulting in potential underestimation of bloom intensity from satellites (Wynne et al., 2010; Kutser et al., 2008). Binding et al. (2018) showed the close agreement between daily lake-average surface Chla and wind speed in LW, suggesting that day-to-day variability in surface Chla seen by the satellite is driven primarily by the repeated mixing and resurfacing of algal material in response to intermittent periods of wind mixing. In LE, the early season high in bloom intensity (Fig. 5c) is driven by an isolated bloom in Sandusky Bay, a protected bay on the southern shore of Lake Erie (Davis et al., 2015). This is a small localized but intense bloom, with spatial extent limited to the Bay itself (an area approximately 143 km^2). It is likely more protected from the wind, which, combined with differences in bloom community composition (Rinta-Kanto and Wilhelm, 2006; Davis et al., 2015; Binding et al., 2019) results in bloom intensity showing little dependence on wind mixing (and so much less daily variability) compared with the exposed open lake bloom of later in the summer.

3.2. Bloom indices

3.2.1. Bloom spatial extent

Fig. 6 presents the seasonal progression of bloom spatial extent for each of the three lakes for the years 2002–11 and 2016–19, along with

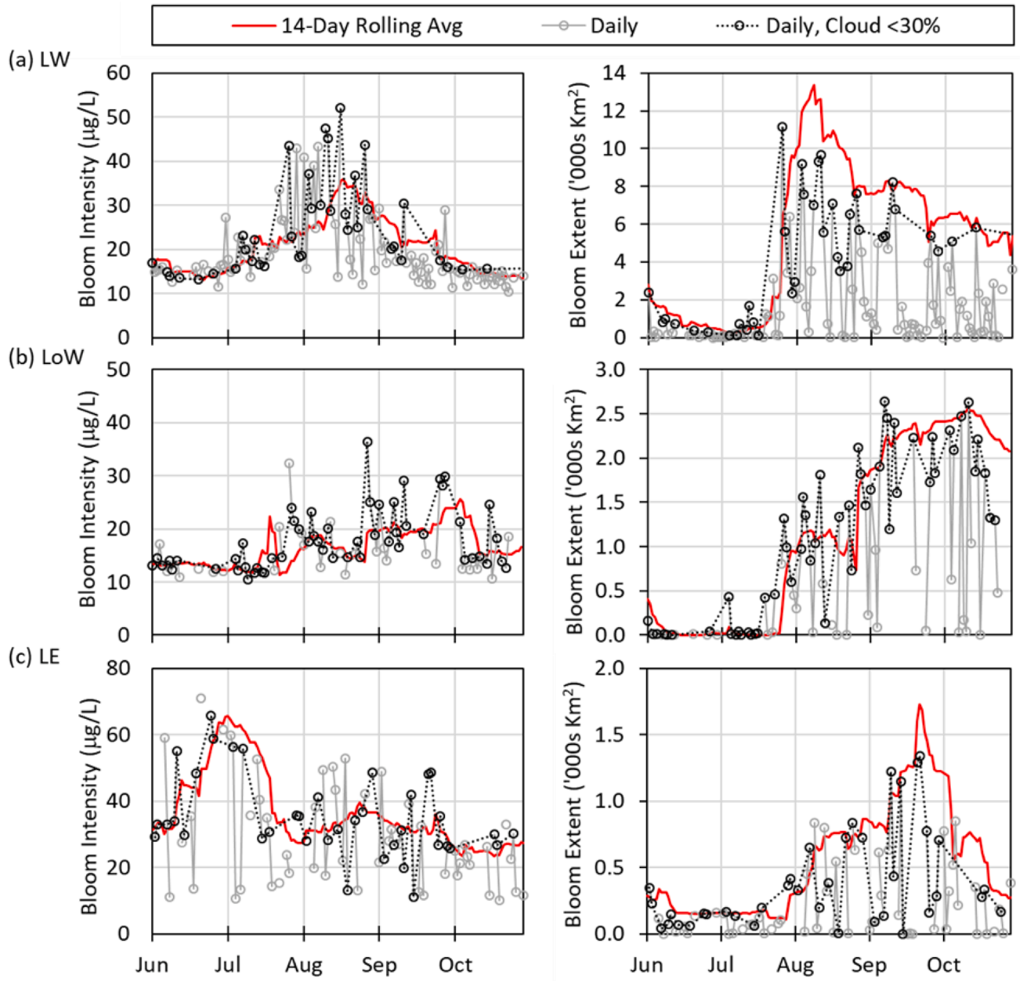

Fig. 5. Bloom intensity and spatial extent for each of the three lakes (a) Lake Winnipeg, (b) Lake of the Woods and (c) Lake Erie, for the 2017 bloom season, showing in open grey: daily average bloom conditions, open black: daily average bloom conditions on days where cloud cover is <30% of the scene, and red: 14-day rolling average bloom conditions.

the season-average and peak bloom extent for each year. The average maximum spatial extent reached by LW algal blooms is 14,811 km^2 (equivalent to 60.3% of the lake area) but varies significantly from year to year, from 6016 km^2 in 2002 to a peak of 21,641 km^2 (88.1%) in 2011. Blooms on LoW exhibit greater consistency from year to year, with an average peak bloom extent of 2619 km^2 (or 67.8% of the lake area), ranging from the smallest bloom of 1354 km^2 (35.1%) in 2019 to its largest bloom of 3070 km^2 (79.5%) in 2006. By comparison, blooms on LE have an average peak extent of 1289 km^2 (just 4.8% of the lake area) but show significant inter-annual variability; at its most extensive, the bloom of 2011 reached a maximum extent of 5257 km^2, covering 19.7% of the lake. The initiation of blooms on LW and LoW appears to be rapid, with the bloom expanding from 25% to 75% of its peak extent in an average of 22 days ($\sigma = 20$) and 25 days ($\sigma = 13$) respectively. For example in July of 2010 the LW bloom grew in size by a factor of 40 from 270 km^2 to more than 10,000 km^2 in just 14 days. In contrast, LE blooms show more gradual expansion, increasing from 25% to 75% of its peak extent over an average of 43 days ($\sigma = 31$).

3.2.2. Bloom intensity

LW average peak bloom intensity was 42.8 µg/L, with the highest annual peak in intensity of 61.1 µg/L in 2005 (Fig. 7a). The highest season-average intensity, however, was observed in 2006 due to the more prolonged bloom that year. Results suggest that LoW experiences significantly lower intensity blooms with an average peak intensity of 30.7 µg/L (Fig. 7b). With the exception of particularly intense blooms in 2003 and 2004, all other recorded blooms peaked at less than 40 µg/L, with a notable reduction in the last four years. A continuing significant downward trend in the average intensity of LoW blooms may be suggestive of the lake responding to historical nutrient load reductions, providing evidence of the effectiveness of nutrient management actions. Observations for LE suggest particularly consistent, more intense blooms, with an average peak bloom intensity of 53.5 µg/L. However, knowing that the early season peak in bloom intensity is driven by the isolated bloom in Sandusky Bay, when data from that bay are removed, the bloom intensity is significantly reduced (Fig. 7c) and the timing shifts to be more consistent with the main in-lake bloom extending from Maumee Bay into the western basin. The average peak bloom intensity of that west basin bloom is then reduced to 38.1 µg/L, more consistent with the range observed on LW and LoW.

3.2.3. Bloom duration

Mapped bloom duration products provide a valuable visualization to identify regions of persistent recurring algal blooms. Fig. 8 presents maps of the 2002–2019 average seasonal (June 1–October 31st) bloom duration for each lake as well as the annual lake-average bloom duration. Annual bloom duration on LW ranged from 19 to 66 days, with an average of 44 days. Imagery identified prolonged blooms in the southern section of the south basin as well as near the north end of the Narrows, where nutrient-rich waters from the turbid south basin first reach more favorable light conditions in the deeper clearer north basin (Binding et al., 2018). Recurring high algal biomass along the north-east shores of

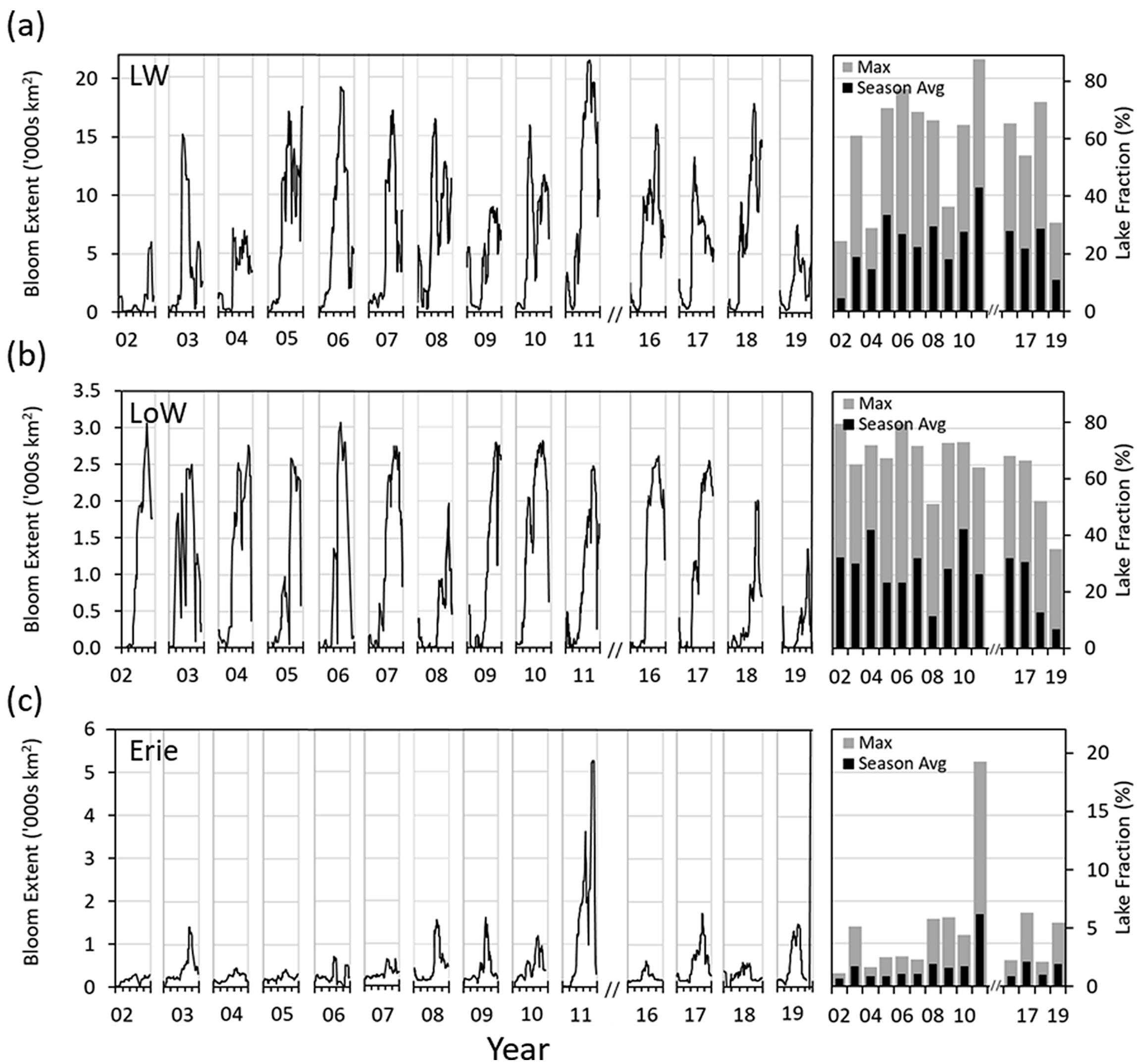

Fig. 6. Bloom spatial extent for each of (a) Lake Winnipeg, (b) Lake of the Woods, and (c) Lake Erie. Left panel showing rolling 14-day average bloom extent for June-Oct each year. Right panel showing the season-average and peak extent for each year.

the north basin is consistent with the predominantly northeastward circulation towards the outflow from the lake at Nelson River (Lévesque and Page, 2011) and with prevailing winds that effectively drives large surface algal scums towards the eastern shoreline. Blooms on LoW ranged in duration from 17 to 61 days, with an average of 47 days. The highest bloom duration occurred mostly in the Big Traverse and Sabaskong Bays (See Fig. 1C) close to the main source of nutrients to the lake via the Rainy River. Of particular note, bloom duration is lowest in Shoal Lake, an isolated embayment in the NW of the LoW system that is the main source of drinking water for the city of Winnipeg. Blooms on LE were significantly shorter in duration, ranging from 16 to 30 days, with an average of 24 days. As is well documented (Stumpf et al., 2012; Michalak et al., 2013), the blooms in LE are typically confined to the west basin, with peak bloom duration found within Sandusky and Maumee Bays (Fig. 1D) consistent with the known major sources of nutrients to the lake (Dove and Chapra, 2015).

3.2.4. Variability in bloom indices

Although providing significant insight on bloom conditions, single bloom indices may not capture the full picture; a bloom might be large but low in biomass, or small and short-lived but extremely high in biomass. Depending on which bloom metric is used, one could potentially reach a different conclusion regarding inter-annual bloom conditions. Here we analysed the consistency in the year-to-year variability of each of the three bloom indices; Intensity, Extent, and Duration. Radar charts (Fig. 9) document the ranking of each bloom index over the 2002–2019 period (where closer to the perimeter represents the highest ranking and closer to the center the lowest ranking). For LW, the mean standard deviation of the rank positions of the three bloom indices each year was 2.3, suggesting significant variability in bloom conditions represented by each index. For example, the highest average intensity bloom of 2006, ranked 7th in average extent but 2nd in peak extent. The bloom of 2016 ranked as one of the lowest intensity, but was the 5th largest bloom of the time series. At its peak, the bloom of 2005 ranked the most intense, while the bloom of 2011 was the most extensive. For LoW, bloom indices showed greater consistency, with the mean standard deviation of the rank positions being 1.5 over the 2002–2019 time-period. As such, the least intense blooms of 2008 and 2019 were also the smallest and the shortest duration. The most intense bloom of 2004 was also the 2nd most extensive, although the bloom of 2003, despite being the longest bloom duration, and 2nd most intense, was only the 7th largest bloom of the record. Lake Erie shows a more complex picture of bloom indices, with a higher standard deviation of the rankings of 3.8. The longest and most intense LE bloom was actually the second smallest bloom of the record in 2005, while the largest bloom of 2011 was the second lowest average intensity. The ranking of the Erie indices, however, is influenced significantly by the effect of the Sandusky Bay blooms; if Sandusky Bay is once again removed, then the largest bloom

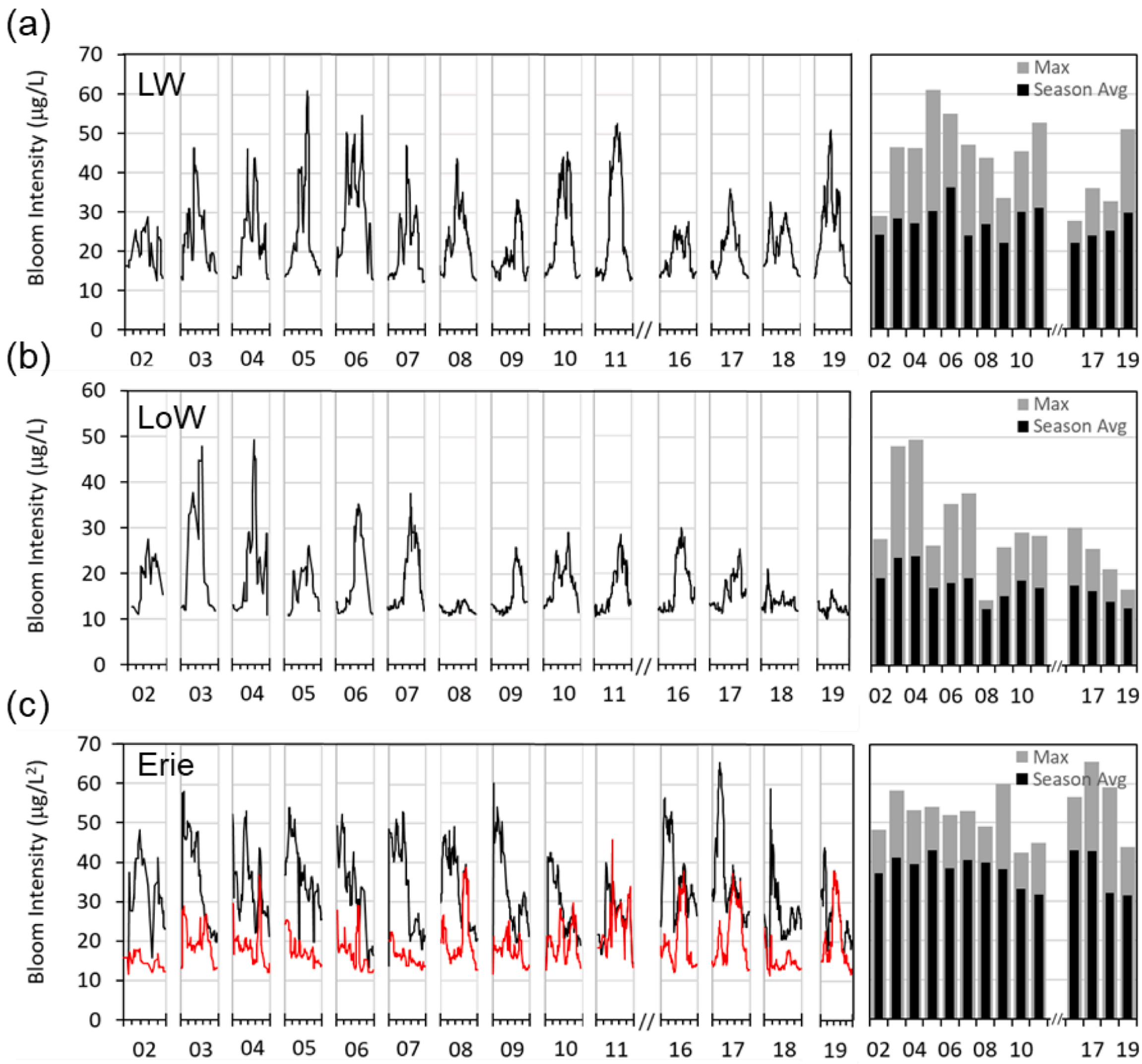

Fig. 7. Bloom intensity for each of (a) Lake Winnipeg, (b) Lake of the Woods, and (c) Lake Erie. Left panel showing rolling 14-day average bloom intensity for June–Oct each year. Right panel showing the season-average and peak intensity for each year. For Lake Erie the red time-series shows the bloom intensity excluding Sandusky Bay and Lake St Clair, therefore is representative of mostly the west basin bloom associated with the Maumee River.

of 2011 is also the most intense and longest in duration and the overall standard deviation is reduced to 2.2.

3.2.5. Annual bloom severity index

In order to account for variability in bloom intensity, spatial extent and duration, an annual bloom severity index (ABSI) is derived according to Eq. (4), as the product of daily bloom intensity and extent averaged for the number of observations over the bloom season, n, from June 1st to October 31st. By taking the average severity over the whole bloom season, the index implicitly accounts for the bloom duration, providing a single combined measure of annual bloom conditions. The bloom severity index could be further normalized by lake area or volume for inter-lake comparisons.

$$ABSI = \sum\nolimits_{1}^{n}(Intensity_{Daily}.Extensity_{Daily})/n \quad (4)$$

Overall, LE exhibits the lowest severity blooms of the three lakes in this study, followed by LoW, with by far the most severe blooms found on LW (Fig. 10). The LW blooms of 2007 and 2017 had the same average bloom intensity and extent, but because the bloom of 2007 was on average 12 days longer, its overall severity was higher than that of 2017. Likewise, the blooms of 2003 and 2017 on LoW were of comparable average extent, but in 2003 the bloom was more intense and longer in duration, therefore considered more severe than that of 2017. The blooms of 2016 and 2017 on LE were the same average intensity, and comparable duration but in 2016 the bloom was half the average size so considerably less severe than 2017. The day of peak bloom severity showed significant variability for each lake over the years (Fig. 10). Blooms on LW peaked in severity as early as August 1 and as late as October 16, with an average day of peak severity on September 1st. On LoW, blooms peaked significantly later; the average peak timing was September 19, with the earliest bloom peaking on August 29 and several years with blooms peaking well into the middle of October. On LE, the average day of peak bloom severity was September 16, but ranged from August 23 in 2016 to October 19 in the severe bloom of 2011.

4. Discussion

4.1. Water quality management implications

Sparse, fragmented datasets and inconsistencies in the timing and location of ground based monitoring surveys of HAB events are major impediments to resolving spatial and temporal trends and developing robust management strategies for their mitigation. Satellite remote sensing has provided the means by which algal blooms can be observed

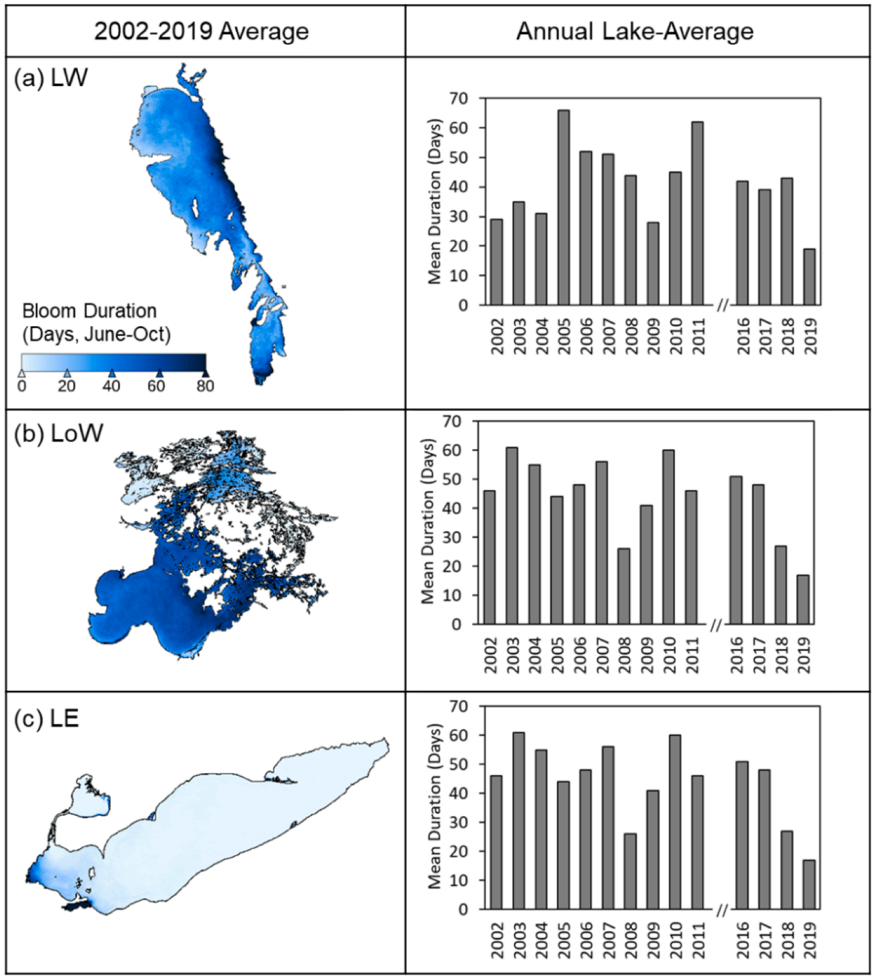

Fig. 8. Mapped cumulative bloom duration from June 1st to October 31st, averaged over 2002–2019, and annual lake-average bloom duration for (a) Lake Winnipeg, (b) Lake of the Woods, and (c) Lake Erie.

with unprecedented frequency and spatial coverage. EOLakeWatch products go a long way to address existing spatial and temporal limitations in ground based monitoring capabilities, delivering frequent, large-scale synoptic observations of lake-wide algal bloom conditions. Mapped bloom products allow for the identification of areas of potential concern, enabling efficiencies in the allocation of field sampling resources and targeted remedial action in areas at higher risk of negative environmental, health or economic impacts. There is both documented and anecdotal evidence of changes in bloom phenology with warming lake temperatures (Vadadi-Fülöp and Hufnagel, 2014; Palmer et al., 2015). Knowledge of the timing of peak bloom severity therefore offers additional improvements in the efficacy of in-lake bloom monitoring programs; existing annual surveys risk capturing peak bloom conditions some years but not others, and as such introducing significant uncertainty in temporal trend assessments from in situ datasets. The frequency of monitoring products afforded by EO therefore allow for robust objective inter-annual and inter-lake comparisons of bloom conditions. Delivery of near-real-time decision-ready information on bloom conditions to stakeholders provides opportunities to mitigate potential detrimental impacts to recreational and drinking waters. Image products can also be integrated into hydro-ecological models to deliver both short-term (Wynne et al., 2013; Soontiens et al., 2019) and seasonal (Stumpf et al., 2016a) algal bloom forecasting capabilities.

Although cyanobacterial concentrations are often positively correlated with microcystins (Paerl and Otten, 2013), the same measure of bloom severity on each lake may not necessarily translate to a comparable risk of bloom toxicity due to seasonal and between-lake variability in phytoplankton community composition and toxigenicity. On Lake Winnipeg, microcystin concentrations in offshore blooms are typically well below recreational and drinking water quality guidelines (Lévesque and Page, 2011). Widespread blooms across southern waters of LoW typically dominated by *Aphanizomenon flos-aquae* have recorded consistently low microcystin concentrations (Watson and Kling, 2017; Zastepa et al., 2017). In contrast, blooms on Lake Erie have been shown to carry significant recurring risk of toxicity with *Microcystis* and *Planktothrix* considered the main toxin producers on the lake (Rinta-Kanto and Wilhelm, 2006; Rinta-Kantoa et al., 2009; Steffen et al., 2014). Cyanobacterial toxins cannot be directly measured by remote sensing due to the lack of any discernible optical signature, and therefore any potential for bloom toxicity determination from space would rely upon proxy-based approaches (Stumpf et al., 2016b). Nevertheless, the combination of bloom indices presented here can help guide the spatial and temporal prioritization of sampling to determine the risk of bloom toxicity. Of note is the fact the date of peak bloom intensity does not necessarily coincide with the date of peak bloom extent, which may have implications for determining the timing of potential toxicity risk.

HABs serve as key indicators of a lake's response to anthropogenic eutrophication, while often also responding to a suite of other watershed, climate, and in-lake drivers (Dale and Beyeler, 2001; Clark et al., 2017). Although cyanobacterial blooms are fundamentally promoted by nutrient loading, climate plays a large role in the spatio-temporal dynamics of blooms in these lakes (Michalak et al., 2013; Watson et al., 2016; Binding et al., 2018), influencing the timing and concentrations of nutrient loads, lake ice cover, frequency and intensity of storm events,

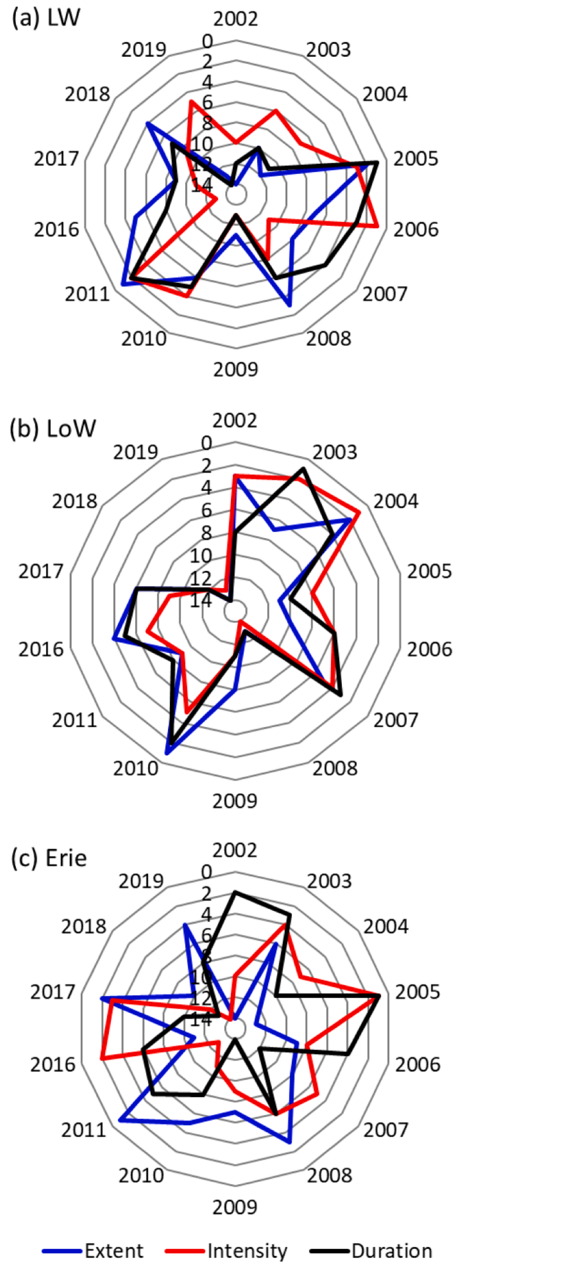

Fig. 9. Ranking of each bloom index over the 14 years of observation, for (a) Lake Winnipeg, (b) Lake of the Woods, and (c) Lake Erie.

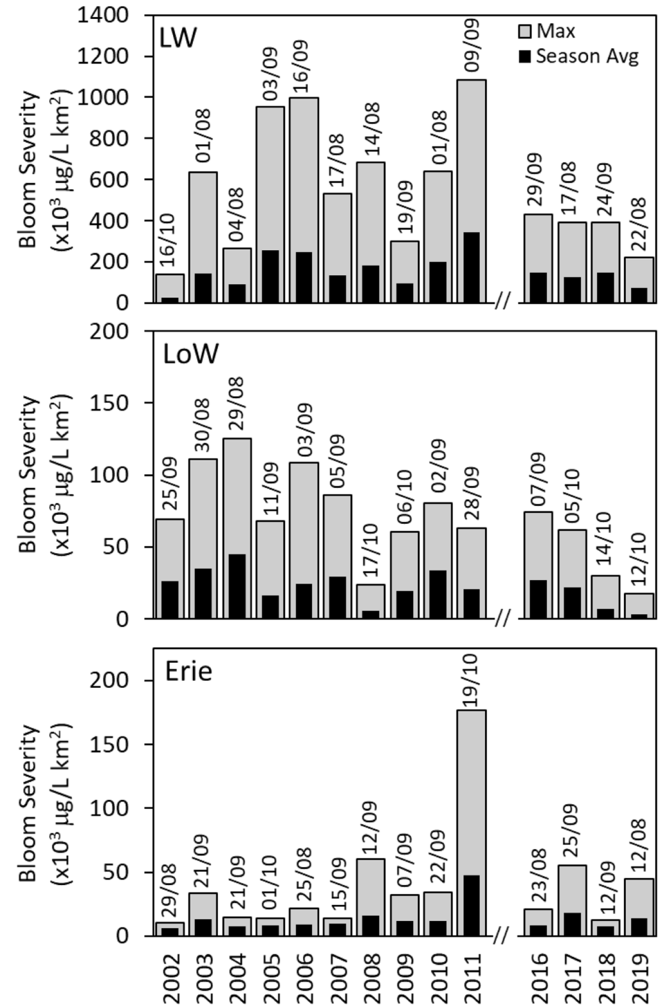

Fig. 10. Season-average and maximum bloom severity for each of (a) Lake Winnipeg, (b) Lake of the Woods and (c) Lake Erie, anotated with the date of maximum bloom severity for each year.

water temperature, stratification and mixing. Numerous studies have shown that Lake Erie blooms correlate well with spring P loads from the Maumee River (Stumpf et al., 2012; Michalak et al., 2013; Stow et al., 2015; Ho and Michalak, 2017), allowing for reasonably robust seasonal predictions of bloom severity (Stumpf et al., 2016a). However, Binding et al. (2018) showed that the response of Lake Winnipeg blooms to annual nutrient loads is confounded by meteorological conditions (wind mixing and summer lake temperature). Similarly, on Lake of the Woods bloom drivers are complicated by the internal loading of legacy nutrients which often obscures annual external load responses. Further understanding bloom dynamics and the processes driving their onset and progression, relies upon the accurate characterization of bloom conditions. Bertani et al. (2017) assessed the coherence of different approaches for algal bloom monitoring on Lake Erie and found that discrepancies in the characterization of seasonal and inter-annual bloom dynamics led to some inconsistencies in the relative importance of select environmental drivers of bloom severity. Variance among the derived bloom indices is shown here to be significant (i.e. the most extensive bloom was not necessarily the longest or most intensive), demonstrating the need for indices to be used in combination or for a single bloom indicator to capture the effects of variable bloom duration, extent and intensity. Collectively, the bloom indices presented here deliver a thorough assessment of bloom conditions, providing consistent, objective metrics with which to carry out analyses of bloom drivers.

Satellite earth observations of blooms have been integral in determining phosphorus load targets required to reduce cyanobacteria blooms on Lake Erie (Stumpf et al., 2016a; Baker et al., 2019). EOLakeWatch products have also been integral in the development and validation of coupled hydrodynamic-ecosystem models used in scenario-based modeling to support ECCC's LoW nutrient target setting (Valipour et al., 2020). The remote sensing indices reported here now provide a comprehensive suite of algal bloom metrics for monitoring the effectiveness of implemented nutrient management practices and guiding adaptive management frameworks across multiple watersheds.

The science and end-user products delivered through EOLakeWatch directly support the Government of Canada's water-resource management mandate and contribute to binational and intergovernmental agreements such as the Canada-Ontario Agreement on Great Lakes Quality and Ecosystem Health, Great Lakes Water Quality Agreement (GLWQA), and Canada–Manitoba Memorandum of Understanding Respecting Lake Winnipeg and the Lake Winnipeg Basin (ECCC, 2018). The Canadian Environmental Sustainability Indicators (CESI) program provides data and information on key environmental issues, including water quality, and is the prime instrument to track Canada's progress on the Federal Sustainable Development Strategy (ECCC, 2013). Adoption of a reliable remote sensing algal bloom indicator and associated target connected to ecosystem management goals would go a long way to addressing the existing scarcity of in situ HAB indicators.

5. Product consistency, uncertainties and limitations

A central requirement for a robust ecological indicator is a consistent and continuous time series of observations. It would be beneficial, therefore, to fill the data gap over the years 2012–15 between the MERIS and OLCI missions in order to more reliably determine temporal trends and lake responses to anthropogenic and environmental drivers. Equivalent algal bloom indices derived from NASA's Moderate Resolution Imaging Spectroradiometer (MODIS), which has neither the same spatial resolution nor the same spectral band properties, are feasible, but require significant validation efforts to ensure continuity in bloom reporting. Moving forward, EO satellite missions are entering a phase of unprecedented data availability; with the launch of the sentinel-3B in 2018 (and future launch of 3C and 3D), the added coverage provided by a constellation of identical sensors will provide exceptional observation capabilities. Furthermore, additional imagery from the Sentinel-2 MultiSpectral Instrument (MSI), with spatial resolution of 10–30 m, has the potential to enhance monitoring of small, localized bloom events and nearshore processes. A benefit of the MCI algorithm as the basis of EOLakeWatch products is the availability of those required wavebands on the MSI allowing the retrieval of consistent chlorophyll and bloom products from this higher resolution imagery. However, the considerable variance documented in bloom indices extracted from daily imagery, brought about by both cloud-induced data gaps and the natural dynamic nature of blooms, highlights the need for frequent observations in order to reliably document any seasonal and long-term trends. We advise caution, therefore, in interpreting time-series observations using satellites such as Landsat and Sentinel-2 MSI with considerably reduced revisit times of 16 and 10 days respectively (Ho et al., 2017; Feng et al., 2020). While offering clear advantages of increased spatial resolution, reduced image frequency may risk misclassifying bloom severity compared with near daily observations offered by OLCI.

There are several sources of potential uncertainty in the satellite retrievals presented, which should be considered when interpreting the derived bloom indices. The threshold for when increased algal biomass constitutes a bloom has been long-debated. While the guideline level of 20,000 cyanobacterial cells per ml (corresponding to 10 μg/L of Chla) set by the World Health Organization (Falconer et al., 1999) is often adopted, variation in this threshold used for defining the bloom on a pixel by pixel basis will clearly have significant impact on derived bloom statistics. For example, the LE bloom extent determined here is in agreement with that of Stumpf et al. (2012) which also reported the peak bloom extent of 2011 to be in excess of 5000 km^2 using the MERIS Cyanobacteria Index (CI). The nominal threshold of the CI equivalent to 20,000 cells/mL (Davis et al., 2019) is consistent with that used here. In contrast, Sayers et al. (2019a) reported substantially lower LE algal bloom extent, which can be explained by the different threshold of Chla (concentrations greater than 18 μg/L) they adopted to define bloom conditions. Furthermore, it's acknowledged that use of a rolling average product will reduce the detection of extremes in bloom indices and high frequency variability. For example, peak bloom extent reported here for LW was on average 18% lower than shown in Binding et al. (2018) for the 2002–2011 period, due to the fact our previous study analysed only whole-lake cloud-free daily images rather than the continuous 14-day rolling averages used here. As additional data sources are included in the processing stream (e.g. Sentinel 3-B OLCI and successors), the minimum number of days required to generate a composite image with complete lake-wide coverage will decrease, thus enabling better detection of real high-frequency bloom variability while minimizing cloud related artifacts. Satellite coverage is considerably greater than is afforded by ground sampling alone but image frequency will undoubtedly result in some bloom occurrences being missed during periods of prolonged cloud cover, a limitation that can be alleviated by integrating image products with statistical (Obenour et al., 2014) or physical (Soontiens et al., 2019) models.

The relationship between Chla and MCI (Eq. (3)) was first developed for LoW (Binding et al., 2011) and has been shown to be broadly consistent for all three lakes (Binding et al., 2018, 2019). Nevertheless, one of the largest sources of uncertainty in the relationship between Chla and satellite-measured MCI is the variability of local inherent optical properties (IOPs) of the dissolved and particulate materials that contribute to the remote sensing reflectance signal. Cyanobacteria blooms often exhibit unique backscatter and absorption features due to the presence of gas vacuoles (Matthews and Bernard, 2013), colonial aggregation (Paerl and Ustach, 1982), or variable pigmentation (Stomp et al., 2007). As such, diversity in phytoplankton community compositions can result in highly variable optical properties as reported in Lake Erie (Binding et al., 2008; O'Donnell et al., 2010; Moore et al., 2017; Sayers et al., 2019b) with significant impact on chlorophyll retrieval algorithms (Binding et al., 2019). Such variability in IOPs may introduce seasonal and/or between-lake bias in derived chlorophyll. Furthermore, the Chl-MCI relationship is known to move towards saturation at Chla ~ 300 μg/L (Binding et al., 2013; Zeng and Binding, 2019), therefore products derived from a linear algorithm may underestimate Chla at extremely high concentrations. Advances in retrieval algorithms brought about by optical water type classifications (Neil et al., 2019), machine-learning (Pahlevan et al., 2020), or hyperspectral imaging (Giardino et al., 2019) provide promise in reducing the uncertainty in derived chlorophyll concentrations moving forward.

6. Conclusions & future directions

Products emanating from EOLakeWatch have advanced significantly Canadian inland water algal bloom monitoring capabilities, making fit-for-purpose end-user products accessible to a wide range of stakeholders in support of lake water quality management. Collectively, the suite of satellite-derived indices developed for three turbid eutrophic lakes, provide objective and consistent measures of bloom conditions that are vital for comprehensive algal bloom monitoring and research. Such products have been integral in providing near-real-time observations of bloom conditions, identifying areas of potential concern, documenting spatio-temporal trends, improving understanding of environmental drivers of blooms, as well as guiding, and monitoring the effectiveness of, nutrient management actions. Future advancement of EOLakeWatch operations, including the expansion of geographic coverage and delivery of an enhanced suite of EO-derived water quality products, promises to augment further opportunities for the integration of EO technologies into Canadian federal solutions for national water quality monitoring, science, and management. Such expansion would enable more comprehensive and more cost-effective large-scale water quality monitoring across Canada. In some regions, EO may be an invaluable complement to in situ monitoring programs, providing synoptic views not possible with ground based observations, while for large swaths of Canadian inland and coastal waters, particularly northern and remote communities, it may be the only monitoring solution. With anecdotal evidence of increasing bloom occurrences in isolated previously pristine waterbodies and northern lakes, reliable remote sensing observations of HAB events may prove invaluable in documenting current, and modeling future, impacts of climate change on Canada's inland water ecosystems.

CRediT authorship contribution statement

C.E. Binding: Conceptualization, Methodology, Validation, Visualization, Investigation. **L. Pizzolato:** Methodology, Software, Data curation, Validation, Visualization, Writing - review & editing. **C. Zeng:** Methodology, Software, Data curation, Validation, Visualization, Writing - review & editing.

Declaration of Competing Interest

The authors declare that they have no known competing financial interests or personal relationships that could have appeared to influence the work reported in this paper.

Acknowledgements

This research was carried out with Environment and Climate Change Canada funding under the programs Lake Winnipeg Basin Program, Great Lakes Protection Initiative and Lake of the Woods Science Plan. The data and imagery used in this manuscript are available on the EOLakeWatch portal at https://www.canada.ca/en/environment-climate-change/services/water-overview/satellite-earth-observations-lake-monitoring.html and the Government of Canada open data portal https://open.canada.ca/data/en/dataset/4d100a02-1494-452f-9f77-84258b26e1cd.

Appendix A. Supplementary data

Supplementary data to this article can be found online at https://doi.org/10.1016/j.ecolind.2020.106999.

References

Anderson, J.P., Paterson, A.M., Reavie, E.D., Edlund, M.B., Rühland, K.M., 2017. An introduction to Lake of the Woods - from science to governance in an international waterbody. Lake Reservoir Manage. 33 (4), 325–334.

Anttila, S., Fleming-Lehtinen, V., Attila, J., Junttila, S., Alasalmi, H., Hällfors, H., Kervinen, M., Koponen, S., 2018. A novel earth observation based ecological indicator for cyanobacterial Blooms. Int. J. Appl. Earth Obs. Geoinf. 64, 145–155.

Baker, D.B., Johnson, L.T., Confesor, R.B., Crumrine, J.P., Guo, T., Manning, N.F., 2019. Needed: Early-term adjustments for Lake Erie phosphorus target loads to address western basin cyanobacterial blooms. J. Great Lakes Res. 45 (2), 203–211.

Berry, M.A., Davis, T.W., Cory, R.M., Duhaime, M.B., Johengen, T.H., Kling, G.W., Marino, J.A., Uyl, P.A.D., Gossiaux, D., Dick, G.J., Denef, V.J., 2016. Cyanobacterial harmful algal blooms are a biological disturbance to Western Lake Erie bacterial communities. Environ. Microbiol. 19 (3), 1149–1162.

Bertani, I., Steger, C.E., Obenour, D.R., Fahnenstiel, G.L., Bridgeman, T.B., Johengen, T. H., Sayers, M.J., Shuchman, R.A., Scavia, D., 2017. Tracking cyanobacteria blooms: do different monitoring approaches tell the same story? Sci. Total Environ. 575, 294–308.

Binding, C.E., Jerome, J.H., Booty, W.G., Bukata, R.P., 2008. Spectral absorption properties of dissolved and particulate matter in Lake Erie. Remote Sens. Environ. 112, 1702–1711.

Binding, C.E., Greenberg, T.A., Jerome, J.H., Bukata, R.P., Letourneau, G., 2011. An assessment of MERIS algal products during an intense bloom in Lake of the Woods. J. Plankton Res. 33, 793–806.

Binding, C.E., Greenberg, T.A., Bukata, R.P., 2013. The MERIS Maximum Chlorophyll Index; its merits and limitations for inland water algal bloom monitoring. J. Great Lakes Res. 39, 100–107.

Binding, C.E., Greenberg, T.A., McCullough, G., Watson, S.B., Page, E., 2018. An analysis of satellite-derived chlorophyll and algal bloom indices on Lake Winnipeg. J. Great Lakes Res. 44 (3), 436–446.

Binding, C.E., Zastepa, A., Zeng, C., 2019. The impact of phytoplankton community composition on optical properties and satellite observations of the 2017 western Lake Erie algal bloom. J. Great Lakes Res. 45 (3), 573–586.

Bridgeman, T.B., Chaffin, J.D., Filbrun, J.E., 2013. A novel method for tracking western Lake Erie Microcystis blooms, 2002–2011. J. Great Lakes Res. 39 (1), 83–89.

Bunting, L., Leavitt, P.R., Simpson, G.L., Wissel, B., Laird, K.R., Cumming, B.F., St. Amand, A., Engstrom, D.R., 2016. Increased variability and sudden ecosystem state change in Lake Winnipeg, Canada, caused by 20th century agriculture. Limnol. Oceanogr. 61, 2090–2107.

Clark, J.M., Schaeffer, B.A., Darling, J.A., Urquhart, E.A., Johnston, J.M., Ignatius, A., Myer, M.H., Loftin, K.A., Werdell, P.J., Stumpf, R.P., 2017. Satellite monitoring of cyanobacterial harmful algal bloom frequency in recreational waters and drinking source waters. Ecol. Ind. 80, 84–95.

Dale, V.H., Beyeler, S.C., 2001. Challenges in the development and use of ecological indicators. Ecol. Indic. 1, 3–10.

Davis, T.W., Bullerjahn, G.S., Tuttle, T., McKay, R.M., Watson, S.B., 2015. Effects of increasing nitrogen and phosphorus concentrations on phytoplankton community growth and toxicity during *Planktothrix* blooms in Sandusky Bay, Lake Erie. Environ. Sci. Technol. 49 (12), 7197–7207.

Davis, T.W., Stumpf, R., Bullerjahn, G.S., McKay, R.M.L., Chaffin, J.D., Bridgeman, T.B., Winslow, C., 2019. Science meets policy: A framework for determining impairment designation criteria for large waterbodies affected by cyanobacterial harmful algal blooms. Harmful Algae 81, 59–64.

DeSellas, A.M., Paterson, A.M., Clark, B.J., Baratono, N.G., Sellers, T.J., 2009. State of the Basin Report for the Lake of the Woods and Rainy River Basin. Environment Canada, March 2009, p. 133.

Dove, A., Chapra, S.C., 2015. Long-term trends of nutrients and trophic response variables for the Great Lakes. Limnol. Oceanogr. 60, 696–721.

ECCC, 2013. Achieving a Sustainable Future: A Federal Sustainable Development Strategy for Canada 2013–2016. http://www.fsds-sfdd.ca/downloads/3130%20-%20Federal%20Sustainable%20Development%20Strategy%202016-2019_pdf (accessed June 2020).

ECCC, 2018. Canada Water Act annual report for April 2017 to March 2018, ISSN 1912-2179, www.canada.ca/en/environment-climate-change/services/water-overview.html (accessed June 2020).

ECCC, 2020. Government of Canada open data catalogue. https://open.canada.ca/data/en/dataset/4d100a02-1494-452f-9f77-84258b26e1cd (accessed June 2020).

EOLakeWatch, 2020. https://www.canada.ca/en/environment-climate-change/services/water-overview/satellite-earth-observations-lake-monitoring.html (accessed June 2020).

Falconer, I, Bartram, J., Chorus, I., Kuiper-Goodman, T., Utkilen, H., Burch, M., Codd, G. A., 1999. SAFE LEVELS AND SAFE PRACTICES, Chapter 5 in: Chorus I., Bartram J. (Eds.), Toxic Cyanobacteria in Water: A Guide to their Public Health Consequences, Monitoring and Management, E & FN Spon, London.

Feng, L., Hou, X., Liu, J., Zheng, C., 2020. Unrealistic phytoplankton bloom trends in global lakes derived from Landsat measurements. EarthArXiv, 6 May 2020.

Giardino, C., Brando, V.E., Gege, P., Pinnel, N., Hochberg, E., Knaeps, E., Reusen, I., Doerffer, R., Bresciani, M., Braga, F., Foerster, S., Champollion, N., Dekker, A., 2019. Imaging spectrometry of inland and coastal waters: state of the art, achievements and perspectives. Surv. Geophys. 40, 401–429.

Gilerson, A.A., Gitelson, A.A., Zhou, J., Gurlin, D., Moses, W., Ioannou, I., Ahmed, S.A., 2010. Algorithms for remote estimation of chlorophyll-a in coastal and inland waters using red and near infrared bands. Opt. Express 18 (23), 24109–24125.

Glibert, P.M., Anderson, D.M., Gentien, P., Granéli, E., Sellner, K.G., 2005. The Global, Complex Phenomena of Harmful Algal Blooms. Oceanography, 18(2) June 2005.

GLWQA, 2012. https://binational.net/2012/09/05/2012-glwqa-aqegl/ (accessed June 2020).

Gower, J., King, S., Borstad, G., Brown, L., 2008. The importance of a band at 709 nm for interpreting water-leaving spectral radiance. Can. J. Remote Sensing 34 (3), 287–295.

Hallegraef, G.M., 1993. A review of harmful algal blooms and their apparent global increase. Phycologia 32 (2), 79–99.

Heiskary, S., Wilson, B., 2008. Minnesota's approach to lake nutrient criteria development. Lake Reservoir Manage. 24 (3), 282–297.

Heisler, J., Glibert, P.M., Burkholder, J.M., Anderson, D.M., Cochlan, W., Dennison, W. C., Dortch, Q., Gobler, C.J., Heil, C.A., Humphries, E., Lewitus, A., Magnien, R., Marshall, H.G., Sellner, K., Stockwell, D.A., Stoecker, D.K., Suddleson, M., 2008. Eutrophication and harmful algal blooms: a scientific consensus. Harmful Algae 8 (1), 3–13.

Ho, J.C., Michalak, A.M., 2017. Phytoplankton blooms in Lake Erie impacted by both long-term and springtime phosphorus loading. J. Great Lakes Res. 43, 221–228.

Ho, J.C., Stumpf, R.P., Bridgeman, T.B., Michalak, A.M., 2017. Using Landsat to extend the historical record of lacustrine phytoplankton blooms: a Lake Erie case study. Remote Sens. Environ. 191, 273–285.

IJC, 2018. International Rainy – Lake of the Woods Watershed Board recommendations submitted by the International Joint Commission to the Governments of Canada and the United States. Accessible at: https://legacyfiles.ijc.org/tinymce/uploaded/Publications/IJC-letter-to-governments-lakeofthewoods-phosphorus-targets-2018-05-03.pdf.

Jetoo, S., Grover, V.I., Krantzberg, G., 2015. The Toledo drinking water advisory: suggested application of the water safety planning approach. Sustainability 7, 9787–9808.

Kahru, M., Elmgren, R., 2014. Multidecadal time series of satellite-detected accumulations of cyanobacteria in the Baltic Sea. Biogeosciences 11, 3619–3633.

Kahru, M., Savchuk, O.P., Elmgren, R., 2007. Satellite measurements of cyanobacterial bloom frequency in the Baltic Sea: interannual and spatial variability. Mar. Ecol. Prog. Ser. 343, 15–23.

Kling, H.J., 1998. A summary of past and recent plankton of Lake Winnipeg, Canada using algal fossil remains. J. Paleolimnol. 19, 297–307.

Kling, H.J., Watson, S.B., McCullough, G.K., Stainton, M.P., 2011. Bloom development and phytoplankton succession in Lake Winnipeg: a comparison of historical records with recent data. Aquatic Ecosyst. Health Manag. 14, 219–224.

Kratzer, S., Kyryliuk, D., Edman, M., Philipson, P., Lyon, S.W., 2019. Synergy of satellite, in situ and modelled data for addressing the scarcity of water quality information for eutrophication assessment and monitoring of Swedish coastal waters. Remote Sensing 11 (17).

Kutser, T., Metsamaa, L., Strömbeck, N., Vahtmäe, E., 2006. Monitoring cyanobacterial blooms by satellite remote sensing. Estuar. Coast. Shelf Sci. 67, 303–312.

Kutser, T., Metsamaa, L., Dekker, A.G., 2008. Influence of the vertical distribution of cyanobacteria in the water column on the remote sensing signal. Estuar. Coast. Shelf Sci. 78, 649–654.

Lévesque, L., Page, E. (Eds.), 2011. State of Lake Winnipeg: 1999–2007, Environment Canada and Manitoba Water Stewardship Report.

Lopez, C.B., Jewett, E.B., Dortch, Q., Walton, B.T., Hudnell, H.K., 2008. Scientific Assessment of Freshwater Harmful Algal Blooms. Washington, DC: Interagency

Working Group on Harmful Algal Blooms, Hypoxia, and Human Health of the Joint Subcommittee on Ocean Science and Technology.
Matthews, M.W., Bernard, S., 2013. Using a two-layered sphere model to investigate the impact of gas vacuoles on the inherent optical properties of Microcystis aeruginosa. Biogeosciences 10 (12), 8139–8157.
Matthews, S., 2016. Satellite technology keeping an eye on South Africa's dams. Water Wheel 15 (1), 24–26.
McCullough, G.K., Page, S., Hesslein, R.H., Stainton, M.P., Kling, H.J., Salki, A., Barber, D.G., 2012. Hydrological forcing of a recent trophic surge in Lake Winnipeg. J. Great Lakes Res. 38, 95–105.
Michalak, A.M., Anderson, E.J., Beletsky, D., Boland, S., Bosch, N.S., Bridgeman, T.B., Chaffin, J.D., Cho, K., Confesor, R., Daloglu, I., DePintoi, J.V., Evans, M.A., Fahnenstiel, G.L., He, L., Ho, J.C., Jenkins, L., Johengen, T.H., Kuod, K.C., LaPorte, E., Liu, X., McWilliams, M.R., Moore, M.R., Posselt, D.J., Richards, R.P., Scavia, D., Steiner, A.L., Verhamme, E., Wright, D.M., Zagorski, M.A., 2013. Record-setting algal bloom in Lake Erie caused by agricultural and meteorological trends consistent with expected future conditions. PNAS 110 (16), 6448–6452.
Miller, T.R., Beversdorf, L.J., Weirich, C.A., Bartlett, S.L., 2017. Cyanobacterial Toxins of the Laurentian Great Lakes, Their Toxicological Effects, and Numerical Limits in Drinking Water. Mar. Drugs. 15 (6), 160.
Mishra, D.R., Kumar, A., Ramaswamy, L., Boddula, V.K., Das, M.C., Page, B.P., Weber, S. J., 2020. CyanoTRACKER: a cloud-based integrated multi-platform architecture for global observation of cyanobacterial harmful algal blooms. Harmful Algae 96, 101828.
Moore, T.S., Mouw, C.B., Sullivan, J.M., Twardowski, M.S., Burtner, A.M., Ciochetto, A. B., McFarland, M.N., Nayak, A.R., Paladino, D., Stockley, N.D., Johengen, T.H., Yu, A.W., Ruberg, S., Weidemann, A., 2017. Bio-optical properties of cyanobacteria blooms in western Lake Erie. Frontiers in Marine Science, 4 (SEP), art. no. 300.
Moses, W.J., Gitelson, A.A., Berdnikov, S., Povazhnyy, V., 2009. Satellite estimation of chlorophyll-a concentration using the red and NIR bands of MERIS; the Azov Sea case study. IEEE Geosci. Remote Sensing Letters 6 (4), 845–849.
Neil, C., Spyrakos, E., Hunter, P.D., Tyler, A.N., 2019. A global approach for chlorophyll-a retrieval across optically complex inland waters based on optical water types. Remote Sens. Environ. 229, 159–178.
Obenour, D., Gronewold, A., Stow, C., Scavia, D., 2014. Using a Bayesian hierarchical model to improve Lake Erie cyanobacteria bloom forecasts. Water Resour. Res. 50 (10), 7847–7860.
O'Donnell, D.M., Effler, S.W., Strait, C.M., Leshkevich, G.A., 2010. Optical characterizations and pursuit of optical closure for the western basin of Lake Erie through in situ measurements. J. Great Lakes Res. 36 (4), 736–746.
Paerl, H.W., Ustach, J.F., 1982. Blue-green algal scums: an explanation for their occurrence during freshwater blooms. Limnol. Oceanogr. 27 (2), 212–217.
Paerl, H.W., Huisman, J., 2008. Blooms Like It Hot. Science 320, 57–58.
Paerl, H.W., Otten, T.G., 2013. Harmful Cyanobacterial Blooms: Causes, Consequences, and Controls. Microb. Ecol. 65, 995–1010.
Pahlevan, N., Smith, B., Schalles, J., Binding, C., Cao, Z., Mae, R., Alikas, K., Kangrof, K., Gurling, D., Hà, N., et al., 2020. Seamless retrievals of chlorophyll-a from Sentinel-2 (MSI) and Sentinel-3 (OLCI) in inland and coastal waters: a machine-learning approach. Remote Sens. Environ. 240, 111604.
Palmer, S.C.J., Odermatt, D., Hunter, P.D., Brockmann, C., Présing, M., Balzter, H., Tóth, V.R., 2015. Satellite remote sensing of phytoplankton phenology in Lake Balaton using 10 years of MERIS observations. Remote Sens. Environ. 158, 441–452.
Paterson, A.M., Rühland, K.M., Anstey, C.V., Smol, J.P., 2017. Climate as a driver of increasing algal production in Lake of the Woods, Ontario, Canada. Lake Reservoir Manag. 33 (4), 403–414.
Pick, F.R., 2016. Blooming algae: a Canadian perspective on the rise of toxic cyanobacteria. Can. J. Fish. Aquat. Sci. 73, 1149–1158.
Rinta-Kanto, J.M., Wilhelm, S.W., 2006. Diversity of microcystin-producing cyanobacteria in spatially isolated regions of Lake Erie. Appl. Environ. Microbiol. 72 (7), 5083–5085.
Rinta-Kantoa, J.M., Konopko, E.A., DeBruyn, J.M., Bourbonniere, R.A., Boyer, G.L., Wilhelm, S.W., 2009. Lake Erie Microcystis: Relationship between microcystin production, dynamics of genotypes and environmental parameters in a large lake. Harmful Algae 8, 665–673.
Reavie, E.D., Edlund, M.B., Andresen, N.A., Engstrom, D.R., Leavitt, P.R., Schottler, S., Cai, M., 2017. Paleolimnology of the Lake of the Woods southern basin: continued water quality degradation despite lower nutrient influx. Lake Reservoir Manage. 33 (4), 369–385. https://doi.org/10.1080/10402381.2017.1312648.
Reinart, A., Kutser, T., 2006. Comparison of different satellite sensors in detecting cyanobacterial bloom events in the Baltic Sea. Remote Sens. Environ. 102, 74–85.
Sayers, M.J., Grimm, A.G., Shuchman, R.A., Bosse, K.R., Fahnenstiel, G.L., Ruberg, S.A., Leshkevich, G.A., 2019a. Satellite monitoring of harmful algal blooms in the Western Basin of Lake Erie: A 20-year time-series. J. Great Lakes Res. 45 (3), 508–521.
Sayers, M.J., Bosse, K.R., Shuchman, R.A., Ruberg, S.A., Fahnenstiel, G.L., Leshkevich, G. A., Stuart, D.G., Johengen, T.H., Burtner, A.M., Palladino, D., 2019b. Spatial and temporal variability of inherent and apparent optical properties in western Lake Erie: Implications for water quality remote sensing. J. Great Lakes Res. 45 (3), 490–507.
Schaeffer, B.A., Bailey, S.W., Conmy, R.N., Galvin, M., Ignatius, A.R., Johnston, J.M., Keith, D.J., Lunetta, R.S., Parmar, R., Stumpf, R.P., Urquhart, E.A., Werdell, P.J., Wolfe, K., 2018. Mobile device application for monitoring cyanobacteria harmful algal blooms using Sentinel-3 satellite Ocean and Land Colour Instruments. Environ. Modell. Software 109, 93–103.
Schindler, D.W., Hecky, R.E., McCullough, G.K., 2012. The rapid eutrophication of Lake Winnipeg: greening under global change. J. Great Lakes Res. 38, 6–13.
Steffen, M.M., Belisle, B.S., Watson, S.B., Boyer, G.L., Wilhelm, S.W., 2014. Status, causes and controls of cyanobacterial blooms in Lake Erie. J. Great Lakes Res. 40 (2), 215–225.
Stow, C.A., Cha, Y., Johnson, L.T., Confesor, R., Richards, R.P., 2015. Long-term and seasonal trend decomposition of maumee river nutrient inputs to western lake erie. Environ. Sci. Technol. 49 (6), 3392–3400.
Smith, R.B., Bass, B., Sawyer, D., Depew, D., 2019. Estimating the economic costs of algal blooms in the Canadian Lake Erie Basin. Harmful Algae 87, 101624.
Soontiens, N., Binding, C., Fortin, V., Mackay, M., Rao, Y.R., 2019. Algal bloom transport in Lake Erie using remote sensing and hydrodynamic modelling: Sensitivity to buoyancy velocity and initial vertical distribution. J. Great Lakes Res. 45 (3), 556–572.
Stomp, M., Huisman, J., Vörös, L., Pick, F.R., Laamanen, M., Haverkamp, T., Stal, L.J., 2007. Colourful coexistence of red and green picocyanobacteria in lakes and seas. Ecol. Lett. 10 (4), 290–298.
Stumpf, R.P., Wynne, T.T., Baker, D.B., Fahnenstiel, G.L., 2012. Interannual variability of cyanobacterial blooms in Lake Erie. PLoS ONE 7 (8), e42444.
Stumpf, R.P., Johnson, L.T., Wynne, T.T., Baker, D.B., 2016a. Forecasting annual cyanobacterial bloom biomass to inform management decisions in Lake Erie. J. Great Lakes Res. 42 (6), 1174–1183.
Stumpf, R.P., Davis, T.W., Wynne, T.T., Graham, J.L., Loftin, K.A., Johengen, T.H., Gossiaux, D., Palladino, D., Burtner, A., 2016b. Challenges for mapping cyanotoxin patterns from remote sensing of cyanobacteria. Harmful Algae 54, 160–173.
Urquhart, E.A., Schaeffer, B.A., Stumpf, R.P., Loftin, K.A., Werdell, P.J., 2017. A method for examining temporal changes in cyanobacterial harmful algal bloom spatial extent using satellite remote sensing. Harmful Algae 67, 144–152.
Vadadi-Fülöp, C., Hufnagel, L., 2014. Climate change and plankton phenology in freshwater: current trends and future commitments. J. Limnol. 73 (1).
Valipour, R., McCrimmon, C., Fong, P., Leon, L., Rao, Yerubandi R., 2020. Phosphorus loads and algal response scenarios: outcomes from the application of a coupled watershed-lake model of Lake of the Woods. International Rainy- Lake of the Woods Watershed Forum, March 11–12 2020, International Falls, Minnesota, USA.
Watson, S.B., Ridal, J., Boyer, G.L., 2008. Taste and odour and cyanobacterial toxins: impairment, prediction, and management in the Great Lakes. Canadian J. Fisheries Aquatic Sci. 65 (8), 1779–1796.
Watson, S.B., Kling, H., 2017. Lake of the Woods phyto- and picoplankton: spatiotemporal patterns in blooms, community composition, and nutrient status. Lake Reservoir Manage. 33 (4), 415–432.
Watson, S.B., Miller, C., Arhonditsis, G., Boyer, G.L., Carmichael, W., Charlton, M.N., Confesor, R., Depew, D.C., Höök, T.O., Ludsin, S.A., Matisoff, G., 2016. The re-eutrophication of Lake Erie: harmful algal blooms and hypoxia. Harmful Algae 56, 44–66.
Winter, J.G., Desellas, A.M., Fletcher, R., Heintsch, L., Morley, A., Nakamoto, L., Utsumi, K., 2011. Algal blooms in Ontario, Canada: increases in reports since 1994. Lake Reservoir Manage. 27, 105–112.
Wynne, T.T., Stumpf, R.P., Tomlinson, M.C., Dyble, J., 2010. Characterizing a cyanobacterial bloom in western Lake Erie using satellite imagery and meteorological data. Limnol. Oceanogr. 55, 2025–2036.
Wynne, T.T., Stumpf, R.P., Tomlinson, M.C., Fahnenstiel, G.L., Dyble, J., Schwab, D.J., Joshi, S.J., 2013. Evolution of a cyanobacterial bloom forecast system in western Lake Erie: development and initial evaluation. J. Great Lakes Res. 39 (S1), 90–99.
Zastepa, A., Watson, S.B., Kling, H., Kotak, B., 2017. Spatial and temporal patterns in microcystin toxins in Lake of the Woods surface waters. Lake Reservoir Manage. 33 (4), 433–443.
Zeng, C., Binding, C.E., 2019. Simulation of mineral sediment impacts on red-NIR algorithms for inland water chlorophyll retrievals. Remote Sensing 11 (19), 2306.